

NEONATAL NEURONAL OVEREXPRESSION OF GLYCOGEN SYNTHASE
KINASE-3 β REDUCES BRAIN SIZE IN TRANSGENIC MICEK. SPITTAELS,^{a1} C. VAN DEN HAUTE,^{a1} J. VAN DORPE,^a D. TERWEL,^a K. VANDEZANDE,^a
R. LASRADO,^a K. BRUYNSEELS,^a M. IRIZARRY,^b M. VERHOYE,^c J. VAN LINT,^d
J. R. VANDENHEEDE,^d D. ASHTON,^e M. MERCKEN,^e R. LOOS,^f B. HYMAN,^b
A. VAN DER LINDEN,^c H. GEERTS^e and F. VAN LEUVEN^{a*}^aExperimental Genetics Group, Department of Human Genetics, K.U. Leuven, Campus Gasthuisberg O&N 06,
B-3000 Leuven, Belgium^bAlzheimer Disease Research Unit, Massachusetts General Hospital-East, CNY 6028, 149 13th St., Charlestown,
MA 02120, USA^cBio-Imaging Lab, Department of Physics, University of Antwerp, Groenenborgerlaan 171, 2020 Antwerpen, Belgium^dDepartment of Biochemistry, K.U. Leuven, Gasthuisberg, B-3000 Leuven, Belgium^eJanssen Research Foundation, B-2340 Beerse, Belgium^fGenetic Epidemiology, Department of Human Genetics, K.U. Leuven, Leuven, Belgium

Abstract—Glycogen synthase kinase-3 β (GSK-3 β) is important in neurogenesis. Here we demonstrate that the kinase influenced post-natal maturation and differentiation of neurons *in vivo* in transgenic mice that overexpress a constitutively active GSK-3 β [S9A]. Magnetic resonance imaging revealed a reduced volume of the entire brain, concordant with a nearly 20% reduction in wet brain weight. The reduced volume was most prominent for the cerebral cortex, without however, disturbing the normal cortical layering. The resulting compacted architecture was further demonstrated by an increased neuronal density, by reduced size of neuronal cell bodies and of the somatodendritic compartment of pyramidal neurons in the cortex. No evidence for apoptosis was obtained. The marked overall reduction in the level of the microtubule-associated protein 2 in brain and in spinal cord, did not affect the ultrastructure of the microtubular cytoskeleton in the proximal apical dendrites. The overall reduction in size of the entire CNS induced by constitutive active GSK-3 β caused only very subtle changes in the psychomotoric ability of adult and ageing GSK-3 β transgenic mice. © 2002 IBRO. Published by Elsevier Science Ltd. All rights reserved.

Key words: glycogen synthase kinase-3 β , microtubule-associated protein 2, microcephaly, transgenic mice.

Glycogen synthase kinase-3 β (GSK-3 β) is a multi-substrate serine/threonine protein kinase that has been implicated in development (Fiol et al., 1994; Ikeda et al., 1998), in cytoskeleton stabilization (Guidato et al., 1996; Guan et al., 1991; García-Pérez et al., 1998; Berling et al., 1994; Sánchez et al., 1996), in the induction of cell processes (Leroy et al., 2000), in cell adhesion (Mackie et al., 1989) and in energy metabolism (Hoshi et al., 1996; Bollen et al., 1998).

A major role for GSK-3 β is evident in neurogenesis, as downstream component of the wingless and Notch signaling pathways that are involved in the development of

the CNS in *Drosophila*, *Caenorhabditis elegans* and mammals (Lendahl, 1998; de la Pompa et al., 1997). GSK-3 β determines cell fate and early development of neuronal tissue as discovered in GSK-3/zeste-white 3 or shaggy mutants of *Drosophila* (Perrimon and Smouse, 1989; Simpson et al., 1988) and confirmed in *Xenopus* (Dominguez et al., 1995; He et al., 1995).

In adult neurons, GSK-3 β regulates stabilization of the cytoskeleton through phosphorylation of neurofilaments and microtubule-associated proteins (MAPs), including protein tau (Avila et al., 1994; Hirokawa et al., 1996; Spittaels et al., 2000; Lucas et al., 2001).

The goal of this study was to investigate *in vivo* the influence of GSK-3 β on the maturation and aging of a mammalian CNS by overexpressing a constitutive active mutant, i.e. GSK-3 β [S9A] (Woodgett, 1991), steered by the mouse thy-1 gene promoter. The thy-1 cell-surface protein is expressed in the thymus but also by neurons that have migrated to their final position and develop dendrites (Morris, 1992). The engineered thy-1 construct used here and in previous studies (Moechars et al., 1999; Spittaels et al., 1999; Tesseur et al., 2000; Van Dorpe et al., 2000) begins expression of the transgene only postnatally and only in neurons.

¹ These authors contributed equally to this work.

*Corresponding author. Tel.: +32-16-345888; fax: +32-16-345871.

E-mail address: fredvl@med.kuleuven.ac.be (F. Van Leuven).

Abbreviations: GSK, glycogen synthase kinase; IA, interaural; IGF-1, insulin-like growth factor-1; M1, primary motor cortex; M2, secondary motor cortex; MAP2, microtubule-associated protein 2; MRI, magnetic resonance imaging; PKB, protein kinase B.

EXPERIMENTAL PROCEDURES

Generation of transgenic mice

Human GSK-3 β [S9A] cDNA (Stambolic and Woodgett, 1994) was ligated in the adapted mouse thy-1 gene vector (Moechars et al., 1996). The replacement of serine at position 9 by alanine, i.e. denoted [S9A], prevents inactivation by phosphorylation by p90 ribosomal S6 kinase, p70 ribosomal S6 kinase and protein kinase B (PKB; Stambolic and Woodgett, 1994). A linearized *PvuI*-*NotI* restriction fragment was micro-injected into 0.5-day FVB/N pre-nuclear mouse embryos and five independent transgenic founder mice were generated by standard methods and maintained in the FVB/N background (Moechars et al., 1999; Spittaels et al., 1999). GSK-3 β protein in brain extracts was estimated by western blotting with a specific monoclonal antibody (tau protein kinase I/ GSK-3 β) (Affiniti, Nottingham, UK). We previously reported an increase in enzymatic activity of about two-fold in strain 5 relative to non-transgenic mice (Spittaels et al., 2000). All experiments reported below were performed with hemizygous human GSK-3 β [S9A] transgenic mice from strain 5 and wild type littermates with FVB/N genetic background (unless stated otherwise). All efforts were made to minimize the number of animals and their suffering. The experiments were carried out in accordance with the European Communities Council Directive of 24 November 1986 (86/609/EEC).

Immunohistochemical localization of the transgene

For immunohistochemical analysis, GSK-3 β [S9A] and wild type littermates were transcardially perfused with 4% paraformaldehyde in phosphate-buffered saline at the age of 5 days post-natally (P5), at P7, at P14 and at adult age. Microtome sections (6 μ m) of paraffin-embedded brain (Bregma -1.46 to -2.54) and spinal cord (thoracolumbal region) were stained with a polyclonal anti-GSK-3 β antibody (Calbiochem, San Diego, CA, USA) as described (Van den Haute et al., 2001).

Macroscopic and microscopic analysis of the CNS

GSK-3 β [S9A] mice ($n=6$) and wild type littermates ($n=7$) were analyzed by magnetic resonance imaging (MRI) protocols described (Fransen et al., 1998; Kooy et al., 1999). Volumes from different brain structures were estimated to find differences between GSK-3 β and wild type mice of 4.5 months old. Brain structures were defined on coronal MR images, according to the Mouse Brain atlas (Franklin and Paxinos, 1997). Their positions were defined in terms of antero-posterior distance to the interaural (IA) line. Image processing was performed using visual C routines and interactive data language. To extract quantitative volume information from a set of *in vivo*-obtained images of the mouse, a semi-automatic 3D segmentation technique (Sijbers et al., 1997) was applied on the 3D MR images data set. The volumes of the total brain, cerebellum, hippocampus (located from IA 2.86 mm to IA -0.08 mm) and part of the cortex were estimated. The cortex volume was calculated as the merged segmented volumes starting from IA 2.86 mm going caudal until the dorsal third ventricle was visual as a spot located IA 1.10 mm. Only the upper half of the cortex (mainly somatosensory cortex, motor cortex, retrosplenial cortex, auditory cortex, posterior parietal association area and visual cortex) was segmented limited by the horizontal brain midline overlaid on each slice.

For wet weight determinations of brain and spinal cord of transgenic and wild type FVB mice ($n=10-30$) at different ages, the entire brain with olfactory bulbs, cerebrum, cerebellum and brain stem, was dissected rostrally to the fossa rhomboidea, while the spinal cord was dissected without the cauda equina.

To determine the area of white and gray matter, paraffin sections ($n=10$) from the cervical intumescence of wild type ($n=4$) and GSK-3 β transgenic mice ($n=5$) (2 months) were stained with Cresyl Violet and analyzed by Bioquant Image analysis system.

Paraffin sections at Bregma -1.94 were stained with Cresyl Violet to investigate the general architecture of the neocortex.

Neuronal density determinations and neuron counts were performed in 16 μ m Nissl stained sagittal brain sections spaced 400 μ m apart spanning one entire hemisphere. Layers II-VI of the entire medial to lateral extent of the neocortex were assessed from a rostral margin = superior to piriform cortex, to a caudal margin = superior to entorhinal cortex. Neuron counts were obtained by a systematic random sampling scheme using approximately 25 optical dissectors consisting of a 50×50 - μ m counting box with extended exclusion lines at $100 \times$ water objective (West and Gundersen, 1990). Neurons were counted if they were not present in the initial plane of focus, but came into focus as the optical plane moved through the tissue. The average coefficient of error of the counting technique was 0.04 (West, 1993). The estimation of total neurons was calculated by multiplying the volume density of the neurons by the volume of the neocortex. The volume of the neocortex (with above described boundaries) was determined by the Cavalieri technique using a Bioquant Image analysis system (Cavalieri, 1966). Layer I was not included in the neocortical volume or neuron count measures. Seven wild type and seven GSK-3 β transgenic mice of 2 months old were used in this study.

The number of primary basal dendrites of pyramidal neurons of layer V was counted on vibratome sections of Golgi-Cox-stained whole mouse brain. The Golgi-Cox impregnation of neurons was performed as described (Gibb and Kolb, 1998). Only well-impregnated cells, showing clearly cell body and basal dendrites, were selected in the primary and secondary motor cortex (M1, M2), retrosplenial granular and agranular cortex (RSG, RSA), posterior parietal association area (Ppta) and primary somatosensory cortex (S1) (Bregma -1.94 mm). Camera lucida drawings were generated of at least 75 pyramidal cortical neurons in vibratome sections (150 μ m) of six wild type and six GSK-3 β transgenic mice.

Cell body areas of pyramidal neurons in cortical areas M1, M2, RSG, RSA, Ppta, S1 and dorsal part of auditory cortex (Bregma -1.94 mm) were measured on paraformaldehyde-fixed brain sections stained with Cresyl Violet. The diameter of apical dendrites of pyramidal neurons in cortical layer V was measured in semi-thin sections (1 μ m) stained with Toluidine Blue. The posterior parietal association cortex (Bregma -2.18 mm) was excised from 40- μ m vibratome sections fixed in paraformaldehyde (4%) with glutaraldehyde (0.1%) and was embedded in epon. Microscope images collected with a 3CCD video camera were analyzed with appropriate software (AIS/C 4.0) (Imaging Research, St. Catharines, ON, Canada).

Ultrathin sections derived from the same brain samples were analyzed by transmission electron microscopy. The number of microtubules in apical dendrites were counted and expressed as mean number per μ m based on four apical dendrites per mouse (three wild type and three GSK-3 β mice) and 15 measurements per dendrite.

Immunohistochemistry and western blot analysis of the CNS

Anesthetized mice were transcardially perfused either with paraformaldehyde (4%, v/v, in PBS) or methacarn and the brain and spinal cord were further treated by standard methods (Spittaels et al., 1999; Van Dorpe et al., 2000). Monoclonal antibodies used were directed to MAP2 (phosphate-independent antibody; Sigma, St. Louis, MO, USA) or to neurofilament proteins: SMI-31 and SMI-32 (Affiniti, Nottingham, UK) and NF-200 (Sigma) (Bregma -1.40 to -2.80).

Apoptosis was detected with the Apoptosis Detection System using the principle of the TUNEL assay (Promega, Madison, WI, USA) and a polyclonal activated caspase-3 antibody (Pharmingen, Heidelberg, Germany) (Bregma -1.40 to -2.80).

Western blotting was performed as described (Spittaels et al., 1999) for GSK-3 β , MAP2 (Sigma, St. Louis, MO, USA), neuron-specific class III β -tubulin (Promega), synaptophysin (DAKO, Glostrup, Denmark) and zinc-finger protein 37 (Zfp-37) (gift of N. Galjart, Rotterdam, The Netherlands) on brain and spinal cord extracts.

Glycogen quantification and detection

Levels of glycogen in cerebrum and cerebellum were enzymatically determined as described (Chan and Exton, 1976). In brief, P14 mice were quick-frozen in 2-methylbutane, pre-cooled by liquid nitrogen. Frozen brains were dissected, cerebellum and cerebrum were separated and both parts were incubated in 2.5 M KOH for 40 min at 90°C. Brain tissue suspensions were spotted on filter paper strips, which were subsequently three times washed in 66% ethanol. Dry filters were incubated with 0.2 mg/ml amyloglucosidase for 90 min at 37°C and glucose was photometrically quantified using a standardized hexokinase method. Age-matched wild type ($n=16$) and GSK-3 β transgenic mice ($n=16$) were analyzed.

As glycogen synthase mRNA, glycogen synthase activity and glycogen content are highest in the cerebellum and are located both in astrocytes and neurons, histological staining of glycogen in Purkinje cells of P14 mice was performed by the periodic acid-Schiff (PAS) reaction on paraffin-embedded sections as described (Cheng et al., 2000). To prevent hydrolysis of glycogen during brain preparation, GSK-3 β ($n=10$) and wild type mice ($n=4$) were quick-frozen in 2-methylbutane and brain was dissected while frozen prior to fixation in 4% paraformaldehyde. The number of PAS-positive Purkinje cells was determined in the vermis.

Cognitive and behavioral tests

Mice were subjected to three cognitive tests: water-maze, E-maze and spontaneous alternation test. The water-maze test was performed with F1 mice, aged 5 months, obtained as offspring from male transgenic GSK-3 β mice with female non-transgenic C57Bl/6J mice as described (Moechars et al., 1999). This strategy yields a homogenous group of hemizygous transgenic F1 offspring, with perfectly matched non-transgenic littermates and overcomes the visual problems of FVB mice (Smith et al., 1997; Moechars et al., 1999). The E-shaped water-maze with hidden platform and a three-arm radial maze (the spontaneous alternation test) were used to determine spatial memory of the same F1 mice at three different ages (254, 345 and 435 days) as non-rewarded exploratory tasks (Sarter et al., 1988). Muscle strength and endurance was measured by the inverted wire grid test (Lamberty and Gower, 1992) and forced swimming test (Spittaels et al., 1999) on GSK-3 β FVB transgenic mice and wild type FVB littermates.

Statistical analysis

A two-tailed Student's *t*-test was applied to volumetric data of the different brain structures determined by MRI and to weights of brain and spinal cord. The Wilcoxon rank-sum test was performed on areas of gray matter, white matter and entire spinal cord in transversal sections, on measurements of neuronal density, on determinations of neocortical volumes obtained by the Cavalieri technique, on the number of primary basal dendrites, on cell body size and diameter of the apical dendrites and on glycogen levels. Analysis of variance and contingency χ^2 tests were used for statistical comparison of groups of mice in the cognitive and behavioral tests. Differences were considered significant if $P < 0.05$.

RESULTS

Temporal and spatial expression of transgenic GSK-3 β [S9A]

Expression of human GSK-3 β [S9A] in brain, as determined by western blotting, was highest in strain GSK-3 β [S9A]-5 (2.5-fold increase) as opposed to strain GSK-3 β [S9A]-1 (1.5-fold increase) compared to non-transgenic mice (Fig. 1a).

Immunohistochemically no differences were observed between wild type and human GSK-3 β [S9A] mice on P5 (Fig. 1b, c). From P7 onwards, expression of the human protein in the brain was widespread in neuronal cell bodies and processes of layer V of the cortex, in the CA regions of the hippocampus (Fig. 1d–g), many nuclei of the thalamus, caudate putamen and in brain stem nuclei. Human GSK-3 β [S9A] was also detected in the gray matter of the spinal cord and in the Purkinje and granular cell layer of the cerebellum (results not shown).

Overexpression of GSK-3 β reduced the volume of brain and spinal cord

By the immunohistochemical analysis, it became obvious to the observers that the brain of adult GSK-3 β [S9A] mice of strains -5 and -1 that were analyzed ($n > 50$) was invariably smaller than that of age-matched non-transgenic mice.

The volume of different brain structures was measured *in vivo* by MR imaging (Fig. 2a). The volume of cerebellum (81%), cerebrum (84%), hippocampus (85%) and cortex (73%) was significantly reduced in GSK-3 β [S9A] transgenic mice relative to age-matched non-transgenic mice. Relative to the volume of the entire brain, only the volume of the cortex is significantly smaller in transgenic mice compared to wild type littermates (Fig. 2b).

Brain wet weight of neonatal non-transgenic and GSK-3 β [S9A]-5 mice aged 1 week was not different, whereas 2 weeks after birth a significant reduction was already evident. The difference increased with age to reach 16.4–18.3% in adult male and female GSK-3 β [S9A]-5 mice, respectively, relative to non-transgenic littermates. In transgenic strain GSK-3 β [S9A]-1, with lower expression of the transgene, reduction in adult brain weight was less than in strain -5, i.e. 12.4–13.2% in males and females, respectively. The body weight in both transgenic strains was not different from that of non-transgenic mice, demonstrating that the microcephaly was specific and not due to a general growth deficit (data not shown).

The human GSK-3 β [S9A] transgene was also expressed in the neurons of the spinal cord and significantly reduced its total wet weight (data not shown). Morphometric analysis of transversal sections of the spinal cord revealed a reduction of 23% of the total area, while white and gray matter were reduced 20 and 26%, respectively, relative to age-matched non-transgenic mice.

Microcephaly in GSK-3 β transgenic mice is due to increased density and reduced size of neurons

Routine hematoxylin/eosin and Cresyl Violet staining demonstrated that the overall cortical architecture in layers I–VI was completely normal (Fig. 3a, b). However, parallel with the reduction in brain volume, the neuronal density in the cortex of the GSK-3 β transgenic mice was significantly increased (+42%). The total number of cortical neurons remained unaltered, as determined stereologically by the optical disector method

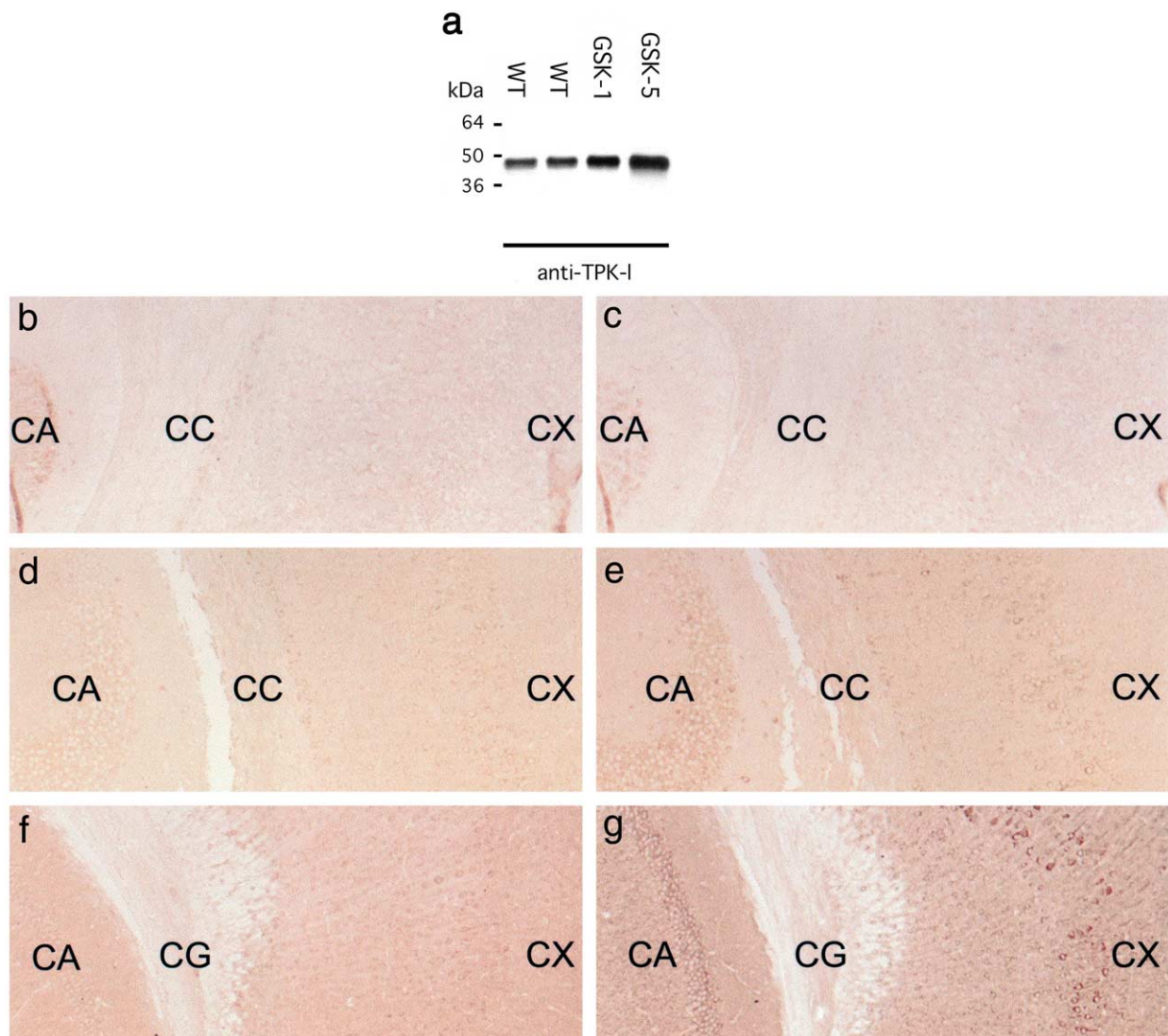


Fig. 1. Analysis of brain of GSK-3 β transgenic mice. (a) Western blotting of brain protein extracts of wild type (WT), GSK-3 β [S9A]-1 (GSK-1) and GSK-3 β [S9A]-5 (GSK-5) transgenic mice with antibody tau protein kinase I (TPKI). (b–g) Immunohistochemistry with antibody TPKI of cortex and hippocampus at P5 (b, c), P7 (d, e) and at adult age (f, g) of GSK-3 β [S9A]-5 transgenic (c, e, g) and non-transgenic (b, d, f) mice. CA: Pyramidal neurons in CA region of the hippocampus, CC: corpus callosum, CG: cingulum, CX: cortex.

and the Cavalieri technique (Fig. 3c–e). The lack of neuronal loss was corroborated by the absence of necrosis and apoptosis, as determined by immunohistochemistry for activated caspase 3 and by TUNEL staining of brain sections of GSK-3 β transgenic mice aged 7, 14 or 70 days (data not shown).

We observed that the distal part of the apical dendrites stained less intensely for MAP2 in cortices of transgenic mice (Fig. 4a, b). In semi-thin sections of the posterior association cortex and of the M1 and M2 the distal (Fig. 4a, b, inset) and proximal (Fig. 4c, d) segments of the apical dendrites were less pronounced and less wide in GSK-3 β transgenic mice than in non-transgenic mice. The diameter of apical dendrites of pyramidal neurons in cortical layer V was significantly reduced (15%) in GSK-3 β transgenic mice (Fig. 4e). Analysis of the distribution of the base diameter of the proximal apical dendrites

demonstrated that 60% were wider than 4 μm in the cortex of non-transgenic mice as opposed to only about 30% in GSK-3 β transgenic mice (Fig. 4f). In addition, careful measurements of cell body area revealed a reduction of 23% in GSK-3 β transgenic mice. In non-transgenic mice, about 80% of pyramidal neurons had a cell body area of $>200 \mu\text{m}^2$, as opposed to only 37% of neurons in GSK-3 β transgenic mice (Fig. 4g, h).

Histochemical and immunochemical analysis of cytoskeletal proteins in brain of adult GSK-3 β mice

Neurofilaments were revealed with phosphorylation-dependent and -independent antibodies, i.e. SMI-32 (Fig. 4k, l) and NF200 (Fig. 4m, n) respectively. In GSK-3 β transgenic mice, the neurofilaments were largely restricted to perikarya and proximal processes of neu-

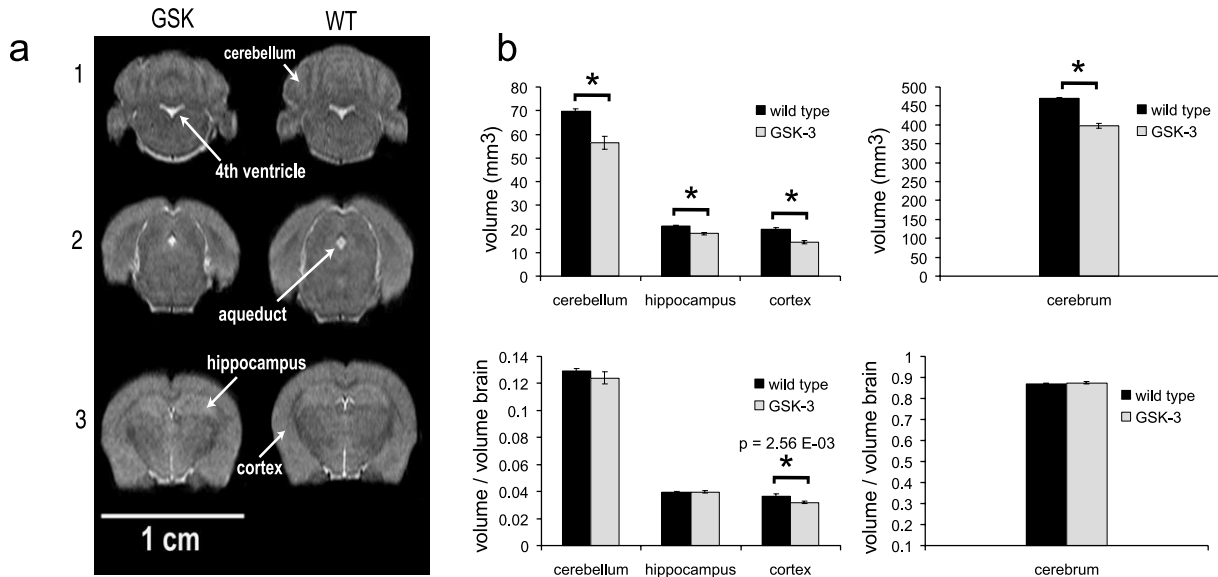


Fig. 2. Microcephaly in GSK-3 β transgenic mice. (a) MRI of brain of a GSK-3 β [S9A]-5 and a wild type mouse. (1) In-vivo coronal MR images through the fourth ventricle, the cerebellum and the pons, (2) through the aqueduct of Sylvius and (3) through hippocampus and cortex. (b) Quantification of the volumes of the different brain structures indicated (cerebellum, hippocampus, cortex and cerebrum) as determined by magnetic resonance imaging (upper panels). Relative to the volume of the entire brain, only the volume of the cortex is significantly smaller in transgenic compared to wild type mice (lower panels) (* $P < 0.001$).

rons as opposed to non-transgenic mice where they extended far into the distal areas of the neurites. Antibody SMI-32 clearly revealed the broader dendrites in non-transgenic mice. In addition, antibody SMI-31 was used to demonstrate preferential staining of neuronal cell

bodies in GSK-3 β transgenic mice, as opposed to mainly distal apical dendrites in non-transgenic mouse brain (Fig. 4i, j).

Camera lucida drawings of Golgi-Cox-impregnated neurons demonstrated that the number of primary

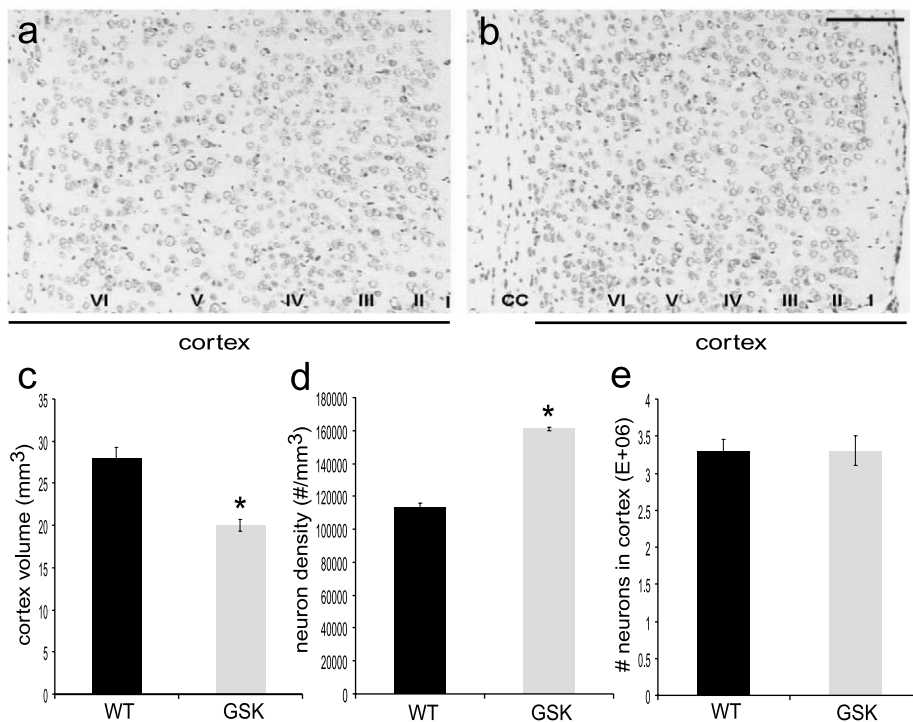
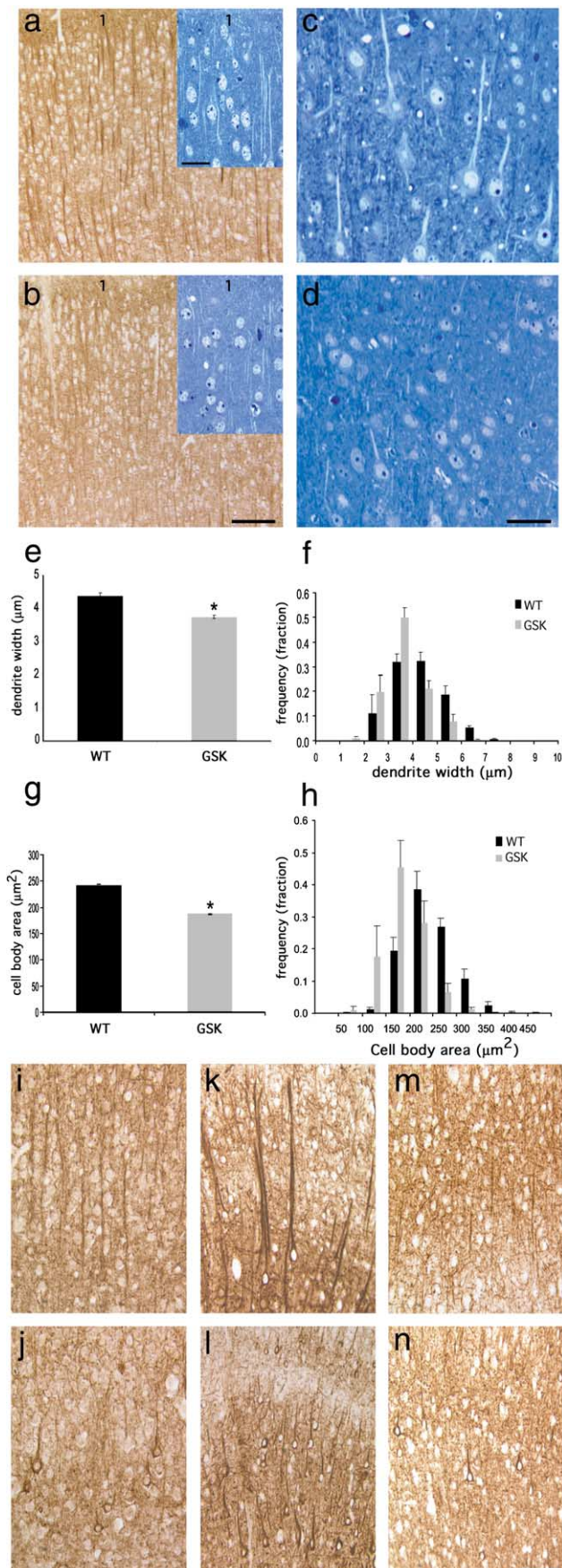


Fig. 3. Increased neuronal density in brain of GSK-3 β [S9A]-5 mice. (a, b) Cresyl Violet staining of the cerebral cortex. Neuronal density is increased in neocortex of a GSK-3 β transgenic mouse (b) compared to a non-transgenic littermate (a). Cortical layers are indicated (I–VI); CC: corpus callosum (scale bar = 100 μ m). (c–e) Histogram representations of cortical volume (c), neuron density (d) and total number of neurons (e) in the cortex of GSK-3 β transgenic mice (GSK, $n = 7$) and non-transgenic littermates (WT, $n = 7$), determined by the disector method and the Cavalieri technique (* $P < 0.05$).



basal dendrites of pyramidal neurons of the fifth layer in the neocortex was not significantly different between non-transgenic and GSK-3 β transgenic mice (data not shown).

Analysis by transmission electron microscopy of the proximal part of the apical dendrite showed the normal appearance of microtubules, while also their density in dendrites did not differ significantly in GSK-3 β transgenic mice from non-transgenic mice, i.e. 0.94 ± 0.08 and 0.87 ± 0.12 microtubules/ μm ($P > 0.05$), respectively (data not shown).

Neuron-specific β -tubulin (N-tubulin) and MAP2 were compared by western blotting in protein extracts from brain of young and adult mice. At P8, the levels of N-tubulin and MAP2 in brain were very similar in mice with either genotype, whereas brain MAP2 levels were already reduced by about 35% in GSK-3 β transgenic mice at P14. In adult GSK-3 β transgenic mice, the MAP2 brain levels further declined to about 50% of those in age-matched non-transgenic mice (Fig. 5). Levels of N-tubulin were only reduced to about 85% of those in non-transgenic mice, whereas the levels of nuclear Zfp-37, a heterochromatin-associated protein in neurons (Payen et al., 1998), and the levels of synaptophysin were both not different in GSK-3 β transgenic mice (Fig. 5).

Histochemical and immunochemical analysis of spinal cord of adult GSK-3 β mice

Immunohistochemical staining for MAP2 of sections of spinal cord revealed a reduced dendritic mass in GSK-3 β transgenic mice compared to wild type littermates. This difference was most outspoken in the ventral and lateral funiculi where the dendrites in the GSK-3 β mice were penetrating less prominent into the white matter compared to those in wild type mice (Fig. 6a, b).

Western blotting for MAP2 revealed a dramatic reduction in the level of MAP2 protein in extracts of the spinal cord from GSK-3 β transgenic mice, whereas the levels of Zfp-37 and of synaptophysin were again not markedly reduced (Fig. 6c). Finally, N-tubulin levels were 25% lower in the spinal cord of GSK-3 β transgenic mice relative to wild type mice (Fig. 6c).

Fig. 4. Reduction of somatodendritic compartment of cortical neurons in GSK-3 β [S9A]-5 transgenic mice. Panels (a–d) are representative for immunohistochemical analysis for MAP2 (a, b) and histochemical staining with Toluidine Blue (c, d; inset in a, b) in the cortex of non-transgenic (a, c) and GSK-3 β transgenic mice (b, d). Measurements of the diameter at the base of apical dendrites (in μm ; panel e, mean \pm S.E.M.; panel f, distribution) and of the cell body area (in μm^2 ; panel g, mean \pm S.E.M.; panel h, distribution) of pyramidal neurons in layers III and V of the neocortex in non-transgenic ($n=5$) and GSK-3 β transgenic mice ($n=5$). For determination of mean dendritic diameter and cell body area, 50–150 pyramidal neurons per mouse were screened ($*P < 0.05$). Brain sections (cortex) from GSK-3 β transgenic mice (j, l, n) and non-transgenic littermates (i, k, m) stained with antibodies SMI-31 (i, j), SMI-32 (k, l) and NF-200 (m, n). Scale bars = 100 μm (a, b), 50 μm (c, d), 45 μm (i–n) or 25 μm (inset, a, b). The first cortical layer, i.e. stratum moleculare, is indicated by the number '1' in (a) and (b).

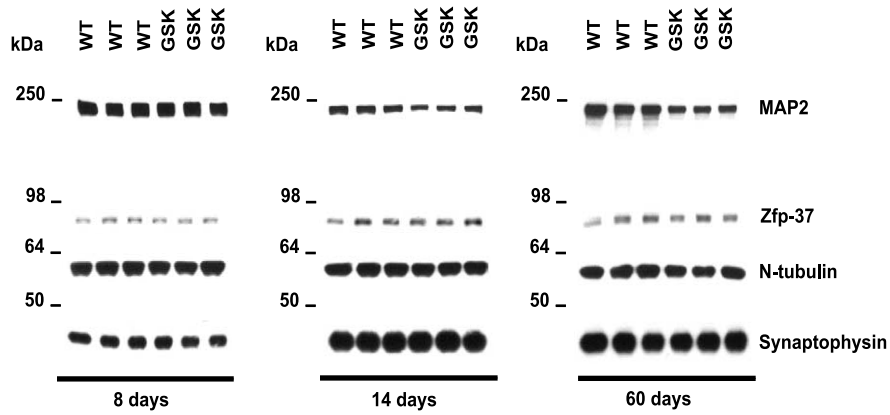


Fig. 5. Prominent reduction of MAP2 in brain extracts of GSK-3 β transgenic mice. Western blotting was performed with specific antibodies specified in the text. Zfp-37 and synaptophysin were used as internal markers. Apparent molecular weight is indicated on the left in kDa. For each genotype three representative mice were analyzed at age as indicated, i.e. 8, 14 and 60 days.

Glycogen levels are normal in brain of GSK-3 β transgenic mice

Glycogen is the largest energy reserve of the brain. As GSK-3 β can inactivate glycogen synthase through phosphorylation, we quantified the glycogen level in the cerebrum and cerebellum of both wild type and transgenic mice. We focused on mice of 14 days old, since around this age brain metabolism shifts from ketone bodies to carbohydrate-based sources of energy and since reduction in brain weight of GSK-3 β transgenic mice is detectable at P14. However, the amount of glycogen in both cerebrum and cerebellum homogenates of GSK-3 β mice was indistinguishable from the levels in brain of wild type littermates (Fig. 7a).

As glycogen synthase mRNA, glycogen synthase activity and glycogen content are highest in the cerebellum (Pellegrini et al., 1996) but also present in glial cells, while GSK-3 β [S9A] expression is limited to neurons, we quantified the ratio of Purkinje cells that contained glycogen in their cytoplasm. The percentage of glycogen-positive Purkinje cells in both genotypes, however, was similar (Fig. 7b, c).

GSK-3 β transgenic mice exhibit subtle psychomotoric deficits

From the GSK-3 β [S9A]-5 transgenic mouse strain we derived a cohort of F1 offspring for testing in the water-maze paradigm (Moechars et al., 1999). The transgenic F1 mice also showed microcephaly (data not shown) but did learn to swim to the submerged platform in the classic water-maze test as efficiently as non-transgenic mice, without major differences in final escape path (Fig. 8a) or latency (Fig. 8b). Only in the first block of tests did the GSK-3 β transgenic mice significantly longer (+37%) than the non-transgenic F1 mice to reach the hidden platform, although the escape path did not differ significantly (Fig. 8b). The subsequent probe trial with the hidden platform removed, demonstrated that all mice, independent of their genetic status, spent the same time exploring the expected quadrant (Fig. 8c). During this 1-min swim test it became obvious, however, that the swim speed of the GSK-3 β transgenic mice was significantly lower (13%) than that of non-transgenic mice (Fig. 8d).

In the classical E-maze test, the number of entries in the arm without the platform was not significantly differ-

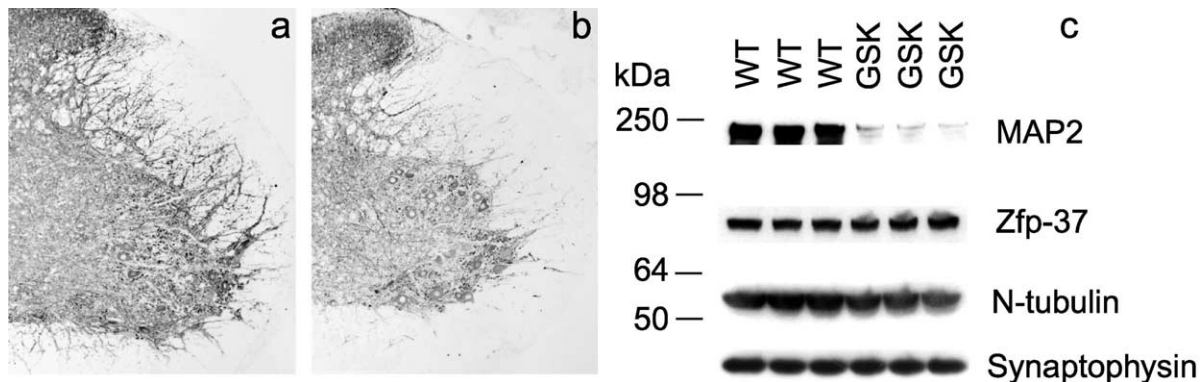


Fig. 6. Prominent reduction of MAP2 in spinal cord of GSK-3 β transgenic mice. (a, b) Reduction of dendritic mass in spinal cord in GSK-3 β [S9A]-5 transgenic mice (b) compared to non-transgenic mice (a) as determined with MAP2. (c) Western blotting of spinal cord extracts of non-transgenic (WT) and GSK-3 β transgenic (GSK) mice showing a prominent reduction of the levels of MAP2, in addition to a modest reduction of N-tubulin. Zfp-37, as internal marker, and synaptophysin were not reduced. Apparent molecular weight is indicated on the left in kDa. For each genotype three representative mice were analyzed.

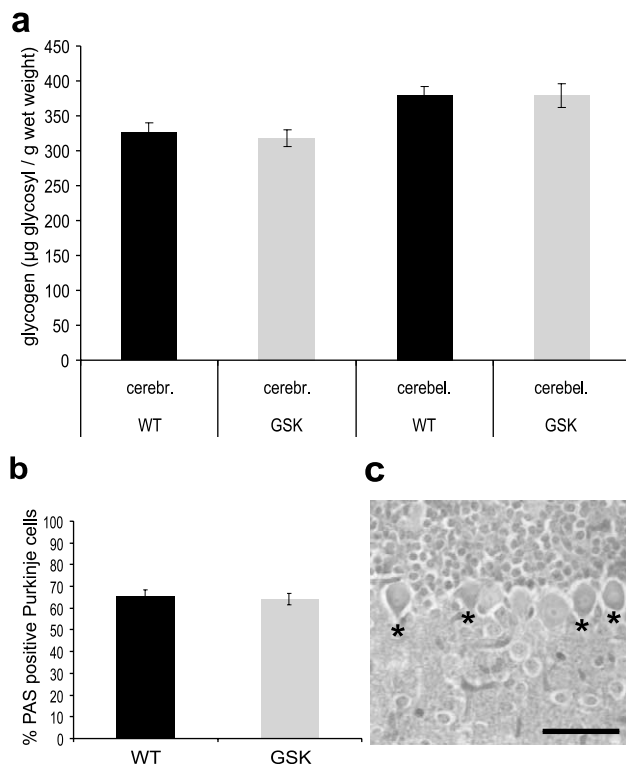


Fig. 7. Normal levels of glycogen in cerebrum and cerebellum of GSK-3 β [S9A]-5 transgenic mice. (a) Mice were killed at P14 and glycogen content in brain tissue derived from both genotypes was compared ($P > 0.5$). (b) Number of PAS positive Purkinje cells (indicated by the asterisk in c), expressed as percent of total number of Purkinje cells in the vermis, was similar in both genotypes. Scale bar = 50 μ m. Shown is mean with S.E.M. cerebr.: cerebrum, cerebel.: cerebellum.

ent for GSK-3 β transgenic mice (Fig. 8e). On the other hand, the latency to swim to the underwater platform was significantly greater for GSK-3 β transgenic mice in all three age groups studied ($P < 0.001$) (Fig. 8f). This lag decreased with the number of trials, concordant with the findings in the Morris water-maze test. In addition, the reversal test resulted for both groups in a significant increase in the number of errors and total latency time (Fig. 8g, h), but no differences between both genotypes could be detected ($P > 0.05$). Moreover, no statistically significant differences were found for the total number of entries and the percentage alternations in the spontaneous alternation test (Fig. 8i, j).

In an inverted wire-grid hang test, significantly less GSK-3 β transgenic mice remained suspended to the grid relative to non-transgenic littermates ($P < 0.05$) (Spittaels et al., 2000).

Combined, all tests indicate only minor or subtle psychomotoric problems of the GSK-3 β transgenic mice despite their more compact brain.

DISCUSSION

The role of GSK-3 β in development within the CNS, although mainly studied in non-mammalian models, predicted that developmental problems were to be expected

by overexpression in the developing CNS. Since we aimed to analyze the role of GSK-3 β in neonatal and adult mouse brain, and to study its function in relation to cognitive capacities during ageing, we opted to overexpress GSK-3 β using an engineered thy-1 gene promoter, which is active only post-natally and only in neurons. Neuronal expression of the thy-1 protein is strictly post-natally and coincides in mice with dendritic outgrowth of migrated neurons after axonal elongation (Morris, 1992; Morris et al., 1992; Bayer and Altman, 1991). The resulting phenotype of the GSK-3 β transgenic mice proved that the strategy did indeed circumvent all major developmental problems. The reduction in size of brain and spinal cord proved not to be a problem for survival and did not cause dramatic alterations of memory function.

Interestingly, the reduced brain size or microcephaly was fully penetrant in the two independent transgenic strains analyzed and was related to the level of overexpression of the GSK-3 β transgene. The reduction in brain volume was reflected by an increased neuronal density, but absence of neuronal loss. The absence of neurodegeneration appeared not consistent with that observed in inducible overexpressing cytomegalovirus-GSK-3 β transgenic mice, at least as indicated by the caspase-3 immunostaining in the dentate gyrus (Lucas et al., 2001). In our thy-1 GSK-3 β [S9A] transgenic mice however, the expression of the human GSK-3 β transgene is constitutive and virtually absent in the dentate gyrus, making direct comparison between the two models impossible.

The physical reason for the microcephaly was found in the significant reduction in the caliber of the proximal and distal part of the apical dendrites and in the size of the cell body area of pyramidal neurons. This reduction in size of the dendritic compartment was underscored by the marked decrease in MAP2 levels and in the more confined distribution of neurofilaments. In addition, the size of the spinal cord was reduced, also concomitant with reduced levels of MAP2. That also spinal cord white matter was decreased was at least partially explained by the reduced dendritic arborization that penetrates into it. No indications were found that GSK-3 β affected axon growth and/or myelination in these transgenic mice, at least not by the unaffected volume of the corpus callosum, as measured by MRI (data not shown). Ultrastructurally, microtubules appeared normal in neurons of GSK-3 β transgenic mice, indicating that the observed minor reduction in the levels of N-tubulin were rather a reflection of the reduced size of the dendritic compartment, although it would also be consistent with a role of GSK-3 β in regulating N-tubulin expression by neurogenin and NeuroD (Marcus et al., 1998).

Although we have collected indications to the underlying problem, the exact mechanism by which GSK-3 β affected the dendritic caliber and cell body area remains to be unraveled. The reduced neuronal and brain size and the decreased MAP2 levels are most likely functionally related. Indeed, primary neurons treated with MAP2 antisense oligonucleotides were smaller and showed reduced neurite outgrowth (Caceres et al., 1992; Sharma

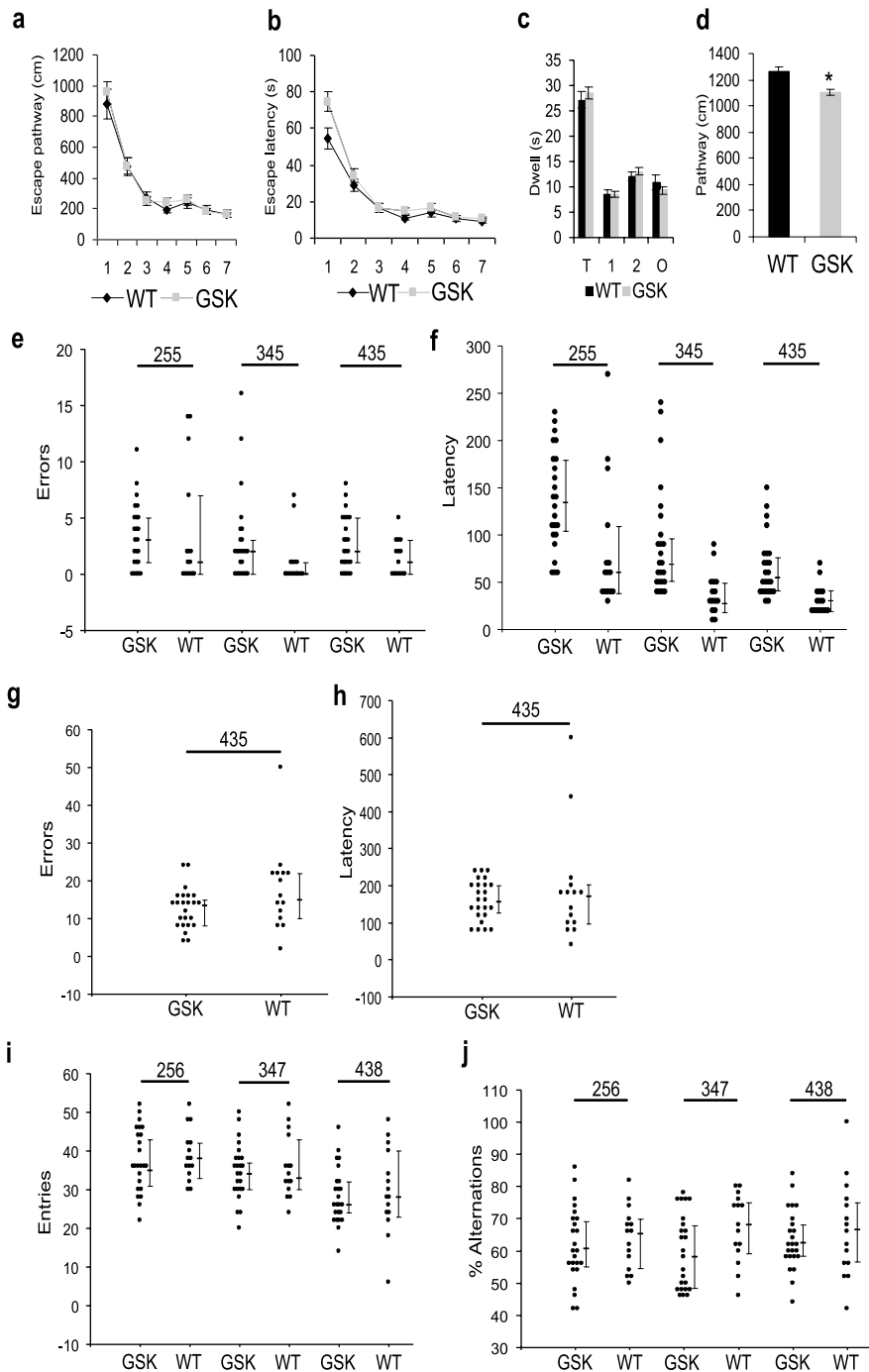


Fig. 8. Psychomotoric tests of GSK-3 β [S9A]-5 transgenic mice. (a-d) Morris water-maze test with mean escape pathway (a) and latency (b) in seven training sessions with hidden platform (place navigation test). Average time spend in each quadrant during a probe test of 1 min with platform removed (c) with quadrants indicated as T: target ($P > 0.05$), 1: first adjacent ($P > 0.05$), 2: second adjacent ($P > 0.05$) and O: opposite ($P > 0.05$). In (d) the mean pathway (in cm) during the 1-min probe test of non-transgenic (WT) and transgenic mice (GSK) ($P < 0.01$) is displayed. (e-h) E-maze test with (e) total number of errors; (f) time in seconds needed to arrive on the platform; (g, h) are results from the reversal E-maze test with (g) total number of errors and (h) total latency time (sum of five trials, in seconds). (i, j) Spontaneous alternation test with (i) number of entries and (j) percent alternation (WT, $n = 15$; GSK, $n = 25$). In (e-j) 255, 256, 345, 347, 435 and 438 denote the age of mice in days.

et al., 1994). Therefore, the demonstrated reduction in MAP2 levels by GSK-3 β overexpression appears functionally pivotal in the reduction of the size of the entire CNS. Nevertheless, GSK-3 β takes part in many and very diverse signal transduction pathways that mediate or can

affect neuronal differentiation (Berezovska et al., 1999; Goold et al., 1999; Sayas et al., 1999; Hall et al., 2000; Li et al., 2000; Redmond et al., 2000). A pathway that likely contributes to the phenotype of the GSK-3 β transgenic mice could be the equivalent of the *Drosophila*

PI3'K/Akt (PKB) signaling pathway (Scanga et al., 2000; Verdu et al., 1999). GSK-3 β is inhibited by phosphorylation at serine 9 by PKB, and our data could position GSK-3 β downstream of PKB as an important determinant in the size of mammalian neurons. Circumstantial evidence is provided by the insulin-like growth factor 1 (IGF-1) that binds to its receptor to activate the PI3'K/PKB/GSK-3 β pathway, in a later phase of neuronal differentiation involving dendrite maturation and myelination. Mice deficient in IGF-1 are characterized by reduced thickness of the cortex and compacting of cell bodies (Beck et al., 1995) and brain weight reduction with smaller neurons with fewer processes (Cheng et al., 2000). The similarity in phenotype of IGF-1 deficient and GSK-3 β overexpressing mice is obvious, and suggests that IGF-1 inactivates the downstream GSK-3 β via activation of PKB. Interestingly, inhibition of PI3'K in human neuroblastoma cells induced neurite retraction via a mechanism which is dependent on GSK-3 activation (Sanchez et al., 2001). Collectively, all the data support the hypothesis that IGF-1/GSK-3 β mediates early post-natal neuronal development and that GSK-3 β determines directly or indirectly the somatodendritic volume of neurons by reducing the levels of MAP2 most likely independent of the amount of glycogen they accumulate.

Most interesting for our ongoing studies of GSK-3 β in the ageing process, was that the reduction in size of the CNS did not cause major cognitive problems in adult mice, as observed in the different test systems, i.e. water-maze, E-maze and spontaneous alternation test.

The reduction in swim speed and the decreased performance on the inverted wire-grid suggest a minor neuromuscular problem. Routine histochemical analysis of muscle revealed no defects or differences between GSK-3 β transgenic and non-transgenic mice, while also no evidence was obtained for effects on cerebellum or on motor neurons in the spinal cord.

In conclusion, constitutively active GSK-3 β caused microcephaly and a higher neuronal density by reducing the volume of the somatodendritic compartment of neurons, i.e. dendrites and cell bodies. The postnatal arrest in neuronal maturation by GSK-3 β did not prevent the GSK-3 β transgenic mice to behave normal in terms of general cognition and ageing with however a minor decline in psychomotoric capability. These conclusions demonstrate that tight regulation of GSK-3 β activity is crucial for the normal maturation of neurons *in vivo*.

Acknowledgements—The intellectual, material and technical contributions of the following scientists are gratefully acknowledged: F. Vandesande, L. Arckens, J. Woodgett, H. Van Der Putten, M. Gilis, C. Kuipéri, I. Laenen, E. Thiry, L. Wouters, H. Van Craenendonck, M. Mahieu, H. Uylings, N. Galjart, M. Bollen, J. Billen. We thank Christina Vochten for administration. This investigation was supported by FWO-Vlaanderen, by the Interuniversity-network for Fundamental Research (IUAP), by the Biotechnology program of the Flemish government (IWT/VLAB/COT-008), by the Flemish Institute for Biotechnology (VIB), by the Janssen Research Foundation (Beerse, Belgium), by a Seed Money grant from COSAT Johnson and Johnson (M.V.), by NFWO-Lotto, by the Rooms-fund, by K.U. Leuven R&D. We thank the K.U. Leuven for continuous support.

REFERENCES

- Avila, J., Dominguez, J., Diaz-Nido, J., 1994. Regulation of microtubule dynamics by microtubule-associated protein expression and phosphorylation during neuronal development. *Int. J. Dev. Biol.* 38, 13–25.
- Bayer, S.A., Altman, J., 1991. *Neocortical Development*. Raven, New York.
- Beck, K.D., Powell-Braxton, L., Widmer, H.R., Valverde, J., Hefti, F., 1995. *Igfl* gene disruption results in reduced brain size, CNS hypomyelination, and loss of hippocampal granule and striatal parvalbumin-containing neurons. *Neuron* 14, 717–730.
- Berezovska, O., McLean, P., Knowles, R., Frosh, M., Lu, F.M., Lux, S.E., Hyman, B.T., 1999. Notch1 inhibits neurite outgrowth in postmitotic primary neurons. *Neuroscience* 93, 433–439.
- Berling, B., Wille, H., Röhl, B., Mandelkow, E.-M., Garner, C., Mandelkow, E., 1994. Phosphorylation of microtubule-associated proteins MAP2a, b and MAP2c at Ser136 by proline-directed kinases *in vivo* and *in vitro*. *Eur. J. Cell Biol.* 64, 120–130.
- Bollen, M., Keppens, F., Stalmans, W., 1998. Specific features of glycogen metabolism in the liver. *Biochem. J.* 336, 19–31.
- Caceres, A., Mautino, J., Kosik, K.S., 1992. Suppression of MAP2 in cultured cerebellar macroneurons inhibits minor neurite formation. *Neuron* 9, 607–618.
- Cavalieri, B., 1966. *Geometria Degli Indivisibili*. Unione Tipografica, Torino.
- Chan, T.M., Exton, J.H., 1976. A rapid method for the determination of glycogen content and radioactivity in small quantities of tissue or isolated hepatocytes. *Ann. Biochem.* 71, 96–105.
- Cheng, C.M., Reinhardt, R.R., Lee, W.-H., Joncas, G., Patel, S.C., Bondy, C.A., 2000. Insulin-like growth factor 1 regulates developing brain glucose metabolism. *Proc. Natl. Acad. Sci. USA* 97, 10236–10241.
- de la Pompa, J.L., Wakeham, A., Correia, K.M., Samper, E., Brown, S., Aguilera, R.J., Nakano, T., Honjo, T., Mak, T.W., Rossant, J., Conlon, R.A., 1997. Conservation of the *Notch* signaling pathway in mammalian neurogenesis. *Development* 124, 1139–1148.
- Dominguez, I., Itoh, K., Sokol, S.Y., 1995. Role of glycogen synthase kinase 3 β as a negative regulator of dorsoventral axis formation in *Xenopus* embryos. *Proc. Natl. Acad. Sci. USA* 92, 8498–8502.
- Fiol, C.J., Williams, J.S., Chou, C.H., Wang, Q.M., Roach, P.J., Andrisani, O.M., 1994. A secondary phosphorylation of CREB³⁴¹ at Ser¹²⁹ is required for the cAMP-mediated control of gene expression. *J. Biol. Chem.* 269, 32187–32193.
- Franklin, K.B.J., Paxinos, G., 1997. *The Mouse Brain in Stereotaxic Coordinates*. Academic, San Diego, CA.
- Fransen, E., D'Hooghe, R., Van Camp, G., Verhoye, M., Sijbers, J., Reyniers, E., Soriano, P., Kamiguchi, H., Willemsen, R., Koekoek, K.E., De Zeeuw, C.I., De Deyn, P.P., Van der Linden, A., Lemmon, V., Kooy, R.F., Willems, P., 1998. L1 knockout mice show dilated ventricles, vermiform hypoplasia and impaired exploration patterns. *Hum. Mol. Genet.* 7, 999–1009.
- García-Pérez, J., Avila, J., Díaz-Nido, J., 1998. Implication of cyclin-dependent kinases and glycogen synthase kinase 3 in the phosphorylation of microtubule-associated protein 1B in developing neuronal cells. *J. Neurosci. Res.* 52, 445–452.
- Gibb, R., Kolb, B., 1998. A method for vibratome sectioning of Golgi-Cox stained whole rat brain. *J. Neurosci. Methods* 79, 1–4.
- Goold, R.G., Owen, R., Gordon-Weeks, P.R., 1999. Glycogen synthase kinase 3 β phosphorylation of microtubule-associated protein 1B regulates the stability of microtubules in growth cones. *J. Cell Sci.* 112, 3373–3384.

- Guan, R.J., Khatra, B.S., Cohlberg, J.A., 1991. Phosphorylation of bovine neurofilament proteins by protein kinase F_A (glycogen synthase kinase 3). *J. Biol. Chem.* 266, 8262–8267.
- Guidato, S., Tsai, L.-H., Woodgett, J., Miller, C.C.J., 1996. Differential cellular phosphorylation of neurofilament heavy side-arm by glycogen synthase kinase 3 and cyclin-dependent kinase-5. *J. Neurochem.* 66, 1698–1706.
- Hall, A.C., Lucas, F.R., Salinas, P.C., 2000. Axonal remodeling and synaptic differentiation in the cerebellum is regulated by WNT-7a signaling. *Cell* 100, 525–535.
- He, H., Saint-Jeannet, J.-P., Woodgett, J.R., Varmus, H.E., Dawid, I.B., 1995. Glycogen synthase kinase-3 and dorsoventral patterning in *Xenopus* embryos. *Nature* 374, 617–622.
- Hirokawa, N., Funakoshi, T., Sato-Harada, R., Kanai, Y., 1996. Selective stabilization of tau in axons and microtubule-associated protein 2C in cell bodies and dendrites contributes to polarized localization of cytoskeletal proteins in mature neurons. *J. Cell Biol.* 132, 667–679.
- Hoshi, M., Takashima, A., Noguchi, K., Murayama, M., Sato, M., Kondo, S., Saitoh, Y., Ishiguro, K., Hoshino, T., Imahori, I., 1996. Regulation of mitochondrial pyruvate dehydrogenase activity by tau protein kinase I/glycogen synthase kinase 3 β in brain. *Proc. Natl. Acad. Sci. USA* 93, 2719–2723.
- Ikeda, S., Kishida, S., Yamamoto, H., Murai, H., Koyama, S., Kikuchi, A., 1998. Axin, a negative regulator of the Wnt signaling pathway, forms a complex with GSK-3 β and β -catenin and promotes the GSK-3 β -dependent phosphorylation of β -catenin. *EMBO J.* 17, 1371–1384.
- Kooy, F., Reyniers, E., Verhoye, M., Sijbers, J., Cras, P., Oostra, B., Willems, P., Van der Linden, A., 1999. Neuroanatomy of the fragile X knockout mouse brain studied using *in vivo* high resolution magnetic resonance imaging (MRI). *Eur. J. Hum. Genet.* 7, 526–532.
- Lamberty, Y., Gower, A.J., 1992. Age-related changes in spontaneous behavior and learning in NMRI mice from middle to old age. *Phys. Behav.* 51, 81–88.
- Lendahl, U., 1998. A growing family of *Notch* ligands. *BioEssays* 20, 103–107.
- Leroy, K., Menu, R., Conreur, J.L., Dayanandan, R., Lovestone, S., Anderton, B.H., Brion, J.P., 2000. The function of the microtubule-associated protein tau is variable modulated by graded changes in glycogen synthase kinase-3 β activity. *FEBS Lett.* 465, 34–38.
- Li, Z., Van Aelst, L., Cline, H.T., 2000. Rho GTPases regulate distinct aspects of dendritic arbor growth in *Xenopus* central neurons *in vivo*. *Nat. Neurosci.* 3, 217–225.
- Lucas, J.J., Hernández, F., Gómez-Ramos, P., Morán, M.A., Hen, R., Avila, J., 2001. Decreased nuclear β -catenin, tau hyperphosphorylation and neurodegeneration in GSK-3 β conditional transgenic mouse. *EMBO J.* 20, 27–39.
- Mackie, K., Sorkin, B.C., Nairn, A.C., Greengard, P., Edelman, G.M., Cunningham, B.A., 1989. Identification of two protein kinases that phosphorylate the neural cell-adhesion molecule, N-CAM. *J. Neurosci.* 9, 1883–1896.
- Marcus, E.A., Kintner, C., Harris, W., 1998. The role of GSK-3 β in regulating neuronal differentiation in *Xenopus laevis*. *Mol. Cell Neurosci.* 12, 269–280.
- Moechars, D., Dewachter, I., Lorent, K., Reversé, D., Baekelandt, V., Naidu, A., Tesseur, I., Spittaels, K., VandenHaute, C., Checler, F., Godaux, E., Cordell, B., Van Leuven, F., 1999. Early phenotypic changes in transgenic mice that overexpress different mutants of amyloid precursor protein in brain. *J. Biol. Chem.* 274, 6483–6492.
- Moechars, D., Lorent, K., De Strooper, B., Dewachter, I., Van Leuven, F., 1996. Expression in brain of amyloid precursor protein mutated in the α -secretase site causes disturbed behavior, neuronal degeneration and premature death in transgenic mice. *EMBO J.* 15, 1265–1274.
- Morris, R., 1992. Thy-1, the enigmatic extrovert on the neuronal surface. *BioAssay* 14, 715–722.
- Morris, R.J., Tiveron, M.C., Xue, G.P., 1992. The relation of the expression and function of the neuronal glycoprotein Thy-1 to axonal growth. *Biochem. Soc. Trans.* 20, 401–405.
- Payen, E., Verkerk, T., Michalovich, D., Dreyer, S.D., Winterpacht, A., Lee, B., De Zeeuw, C.I., Grosveld, F., Galjart, N., 1998. The centromeric/nucleolar chromatin protein Zfp-37 may function to specify neuronal nuclear domains. *J. Biol. Chem.* 273, 9099–9109.
- Pellegrini, G., Rossier, P., Magistretti, P.J., Martin, J.-L., 1996. Cloning, localization and induction of mouse brain glycogen synthase. *Mol. Brain Res.* 38, 191–199.
- Perrimon, N., Smouse, D., 1989. Multiple functions of a *Drosophila* homeotic gene, *zeste-white 3*, during segmentation and neurogenesis. *Dev. Biol.* 135, 287–305.
- Redmond, L., Oh, S.-R., Hicks, C., Weinmaster, G., Gosh, A., 2000. Nuclear Notch 1 signaling and the regulation of dendritic development. *Nat. Neurosci.* 3, 30–40.
- Sánchez, C., Tompa, P., Szücs, K., Friedrich, P., Avila, J., 1996. Phosphorylation and dephosphorylation in the proline-rich C-terminal domain of microtubule-associated protein 2. *Eur. J. Biochem.* 241, 765–771.
- Sanchez, S., Sayas, C.L., Lim, F., Diaz-Nido, J., Avila, J., Wandosell, F., 2001. The inhibition of phosphatidylinositol-3-kinase induces neurite retraction and activates GSK3. *J. Neurochem.* 78, 468–481.
- Sarter, M., Bodewitz, G., Stephens, D.N., 1988. Attenuation of scopolamine-induced impairment of spontaneous alteration behaviour by antagonist but not inverse agonist and agonist beta-carbolines. *Psychopharmacology* 94, 491–495.
- Sayas, C.L., Moreno-Flores, M.T., Avila, J., Wandosell, F., 1999. The neurite retraction induced by lysophosphatidic acid increases Alzheimer's disease-like tau phosphorylation. *J. Biol. Chem.* 274, 37046–37052.
- Scanga, S.E., Ruel, L., Binari, R.C., Snow, B., Stambolic, V., Bouchard, D., Peters, M., Calvieri, B., Mak, T.W., Woodgett, J.R., Manoukian, A.S., 2000. The conserved PI3'K/PTEN/Akt signalling pathway regulates both cell size and survival in *Drosophila*. *Oncogene* 19, 3971–3977.
- Sharma, N., Kress, Y., Shafit-Zagardo, B., 1994. Antisense MAP-2 oligonucleotides induce changes in microtubule assembly and neuritic elongation in pre-existing neurites of rat cortical neurons. *Cell Motil. Cytoskeleton* 27, 234–247.
- Sijbers, J., Scheunders, P., Verhoye, M., Van der Linden, A., Van Dyck, D., Raman, E., 1997. Watershed-based segmentation of 3D MR data for volume quantization. *Magn. Reson. Imaging* 15, 679–688.
- Simpson, P., El Messal, M., Moscoso de Prado, J., Ripoll, P., 1988. Stripes of positional homologies across the wing blade of *Drosophila melanogaster*. *Development* 103, 391–401.
- Smith, D.J., Stevens, M.E., Sudanagunta, S.P., Bronson, R.T., Makhinson, M., Watabe, A.M., O'Dell, T.J., Fung, J., Weier, H.-U.G., Cheng, J.-F., Rubin, E.M., 1997. Functional screening of 2 Mb of human chromosome 21q22.2 in transgenic mice implicates minibrain in learning defects associated with Down syndrome. *Nat. Genet.* 16, 28–36.
- Spittaels, K., Van den Haute, C., Van Dorpe, J., Bruynseels, K., Vandezande, K., Laenen, I., Geerts, H., Mercken, M., Sciot, R., Van Lommel, A., Loos, R., Van Leuven, F., 1999. Prominent axonopathy in the brain and spinal cord of transgenic mice overexpressing four-repeat human tau protein. *Am. J. Pathol.* 155, 2153–2165.
- Spittaels, K., Van den Haute, C., Van Dorpe, J., Geerts, H., Mercken, M., Bruynseels, K., Lasrado, R., Vandezande, K., Laenen, I., Boon, T., Van Lint, J., Vandenheede, J., Moechars, D., Loos, R., Van Leuven, F., 2000. Glycogen synthase kinase-3 β phosphorylates protein tau and rescues the axonopathy in the central nervous system of human four-repeat tau transgenic mice. *J. Biol. Chem.* 275, 41340–41349.
- Stambolic, V., Woodgett, J.R., 1994. Mitogen inactivation of glycogen synthase kinase-3 β in intact cells via serine 9 phosphorylation. *Biochem. J.* 303, 701–704.

- Tesseur, I., Van Dorpe, J., Spittaels, K., Van den Haute, C., Moechars, D., Van Leuven, F., 2000. Expression of human apolipoprotein E4 in neurons causes hyperphosphorylation of protein Tau in the brain of transgenic mice. *Am. J. Pathol.* 156, 951–964.
- Van den Haute, C., Spittaels, K., Van Dorpe, J., Lasrado, R., Vandenzande, K., Laenen, I., Geerts, H., Van Leuven, F., 2001. Coexpression of human cdk5 and its activator p35 with human protein tau in neurons in brain of triple transgenic mice. *Neurobiol. Dis.* 8, 32–44.
- Van Dorpe, J., Smeijers, L., Dewachter, I., Nuyens, D., Spittaels, K., Van den Haute, C., Mercken, M., Moechars, D., Laenen, I., Kuiperi, C., Bruynseels, K., Tesseur, I., Loos, R., Vanderstichele, H., Checler, F., Van Leuven, F., 2000. Prominent cerebral amyloid angiopathy in transgenic mice overexpressing the London mutant of human APP in neurons. *Am. J. Pathol.* 157, 1283–1298.
- Verdu, J., Buratovich, M.A., Wilder, E.L., Birnbaum, M.J., 1999. Cell-autonomous regulation of cell and organ growth in *Drosophila* by Akt/PKB. *Nat. Cell Biol.* 1, 500–506.
- West, M., 1993. New stereologic methods for counting neurons. *Neurobiol. Aging* 14, 275–285.
- West, M.J., Gundersen, H.J.G., 1990. Unbiased stereological estimation of the number of neurons in the human hippocampus. *J. Comp. Neurol.* 296, 1–22.
- Woodgett, J.R., 1991. A common denominator linking glycogen metabolism, nuclear oncogenes and development. *TIBS* 16, 177–181.

(Accepted 18 April 2002)